THE JOURNAL OF PHYSICAL CHEMISTRY A

Article

pubs.acs.org/JPCA

Infrared Spectra and Electronic Structure Calculations for NN Complexes with U, UN, and NUN in Solid Argon, Neon, and Nitrogen

Lester Andrews,* Xuefeng Wang,† Yu Gong, and Gary P. Kushto‡

Department of Chemistry, Box 400319, University of Virginia, Charlottesville, Virginia 22904-4319, United States

Bess Vlaisavljevich and Laura Gagliardi

Department of Chemistry and Minnesota Supercomputing Institute, University of Minnesota, 207 Pleasant Street SE, Minneapolis, Minnesota 55455-0431, United States

Supporting Information

ABSTRACT: Reactions of laser-ablated U atoms with N_2 molecules upon codeposition in excess argon or neon at 4 K gave intense NUN and weak UN absorptions. Annealing produced progressions of new absorptions for the $UN_2(N_2)_{1,2,3,4,5}$ and $UN(N_2)_{1,2,3,4,5,6}$ complexes. The neon-to-argon matrix shift decreases with increasing NN ligation and therefore the number of noble gas atoms left in the primary coordination sphere around the NUN molecule. Small matrix shifts are observed when the secondary coordination layers around the primary $UN_2(N_2)_{1,2,3,4,5}$ and $UN(N_2)_{1,2,3,4,5,6}$ complexes are changed from neon-to-argon to nitrogen. Electronic structure, energy, and frequency calculations provide support for the identification of these complexes and the characterization of the N≡U≡N and U≡N core molecules as terminal uranium nitrides. Codeposition of U with pure nitrogen produced the saturated $U(NN)_7$ complex, which UV irradiation converted to the $NUN(NN)_5$ complex with slightly lower frequencies than found in solid argon.

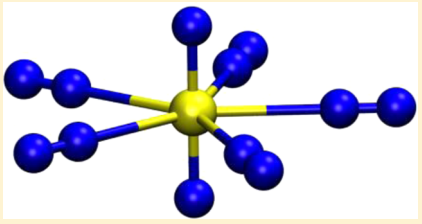

INTRODUCTION

Uranium forms multiple bonds with main-group elements, which is of considerable research importance. Numerous U═O bonds but fewer U═NX and U═CX_2 bonds are known. Imido (U═NX) and N−U−N molecular linkages have been prepared,[1−4] and evidence for the formation of a transient terminal uranium nitride complex following the photolysis of a uranium azide in toluene solution has been presented.[5] The synthesis and structure of bulk uranium nitride complexes is a very important topic: ligand-stabilized U(V) and U(VI) complexes have recently been prepared, and terminal U≡N bond of lengths 1.825(15) and 1.799(7) Å have been measured.[6,7] In addition, thermally stable uranium dinitrogen complexes are of interest for a possible role in nitrogen fixation.[8]

Three solid uranium nitrides are known (UN, UN_2, and U_2N_3),[9] and numerous terminal uranium nitride molecular species have been produced and identified in matrix isolation experiments.[10−17] The simple linear N≡U≡N molecule, which is isoelectronic with the uranyl dication, was observed quite some time ago,[10−13] and it has been characterized only by matrix infrared spectroscopy. Green and Reedy sputtered an 0.5% N_2/argon mixture through a uranium hollow cathode and observed both UN and NUN in the effluent after trapping of the gas stream.[10] Later work in our laboratory employed laser-ablated uranium for reaction with N_2 in argon upon condensation and found an increased yield of NUN plus $(NUN)(NN)_x$ complexes, particularly after UV irradiation, and the reaction in pure N_2 produced additional saturated $NUN(NN)_x$ and $(UN)(NN)_x$ complexes.[11−13]

It must be pointed out here that the authors of the transient terminal uranium nitride work claimed in 2010 to have discovered the first terminal uranium nitride and employed the first photochemistry to produce a transient uranium nitride.[5] This claim overlooked the matrix isolation investigations of Green and Reedy in 1976 and those from our laboratory in 1993, 1997, 1998, and 1999 where U≡N and N≡U≡N were first observed, their absorptions increased markedly by U excitation through UV irradiation, and they were reported without fanfare.[10−14]

Viswanathan et al. laser-ablated UO_2 into argon, which gave the same species as laser-ablated U + O_2 in argon produced in our first excursion into U atom chemistry, and also into N_2-doped argon and into pure N_2, where they observed species such as NUO, the major product of our U + NO reaction.[13−15] The most interesting difference was the observation of NUO and its $(NN)_x$ complexes, but a number of their assignments must be modified, and they will be addressed here.

Recent reactions of U with N_2 and H_2 mixtures in our laboratory produced the N≡U═N−H molecule, which contains both triple and double uranium−nitrogen bonds, as characterized by the infrared spectrum and theoretical computations.[16]

Received: March 26, 2014
Revised: May 15, 2014
Published: May 30, 2014

   dx.doi.org/10.1021/jp501637j | J. Phys. Chem. A 2014, 118, 5289−5303

The subsequent reaction of U and NF_3 produced only the most stable $N{\equiv}UF_3$ product.[17] We have published a short description of the dinitrogen complexes of NUN and UN formed upon sample annealing in recent argon matrix investigations of U and N_2 reactions.[18] The most important new information on the terminal nitride UN is the observation of rotationally resolved optical transitions of supersonically cooled UN, which provided a ground-state UN bond length of 1.7650(12) Å.[19]

It is noteworthy that small molecules such as $N{\equiv}U{=}O$, $NH{=}UH_2$, $N{\equiv}UF_3$, $CH_2{=}UH_2$, $U{\equiv}C$, $C{\equiv}U{\equiv}C$, and the molecular cation $N{\equiv}U{\equiv}O^+$, which is isoelectronic with $N{\equiv}U{\equiv}N$, have been synthesized in small quantities and characterized in matrix isolation experiments, which demonstrates the utility of the laser ablation method for generating reactive uranium atoms.[13−17,20−24]

Our first reaction of laser-ablated U atoms and N_2 trapped only the NUN product, presumably because the substrate temperature of 12 K was too high for rapid quenching of the argon diluent to isolate the diatomic UN molecule and prevent its further reaction.[11] Subsequent laser ablation work necessitated a re-examination of this system, and the weak UN absorptions[16] were observed upon trapping in solid argon at 4 K. After sample deposition, annealing produced a progression of new absorptions for the $UN(N_2)_{1,2,3,4,5,6}$ set of complexes whose identification was facilitated by density functional theory (DFT) frequency and energy calculations.[18] Additional experiments were performed to locate the neon matrix counterpart of UN and to compare the $NUN(NN)_x$ complexes in solid argon and neon. Experiments at higher nitrogen concentrations were also done to help determine the number of dinitrogen molecules, x, in the primary coordination sphere around the uranium center and to probe the secondary coordination layers. In this process we found evidence for dinitrogen complexes with the atomic U center, which will be discussed here as well.

Earlier work on reactions of laser-ablated Th, Mo, and W atoms with dinitrogen produced the diatomic MN and triatomic NMN molecules in addition to $Th(NN)_2$ and the octahedral $M(NN)_6$ complexes.[25] DFT calculations suggested bent structures for these transition-metal dinitrides, in contrast to linear $N{=}Th{=}N$ and $N{\equiv}U{\equiv}N$.[11,12,18]

Extensive work has been done with the isoelectronic CUO molecule (prepared from U insertion with CO) in argon and neon matrices, and noble gas substitution experiments have shown that four noble gas atoms coordinate with the uranium center in CUO.[26−29] This serves as a starting model for $NUN(NN)_x$ complexes. We must also consider the possibility that five NN molecules might coordinate to the U center in NUN based on recent gas-phase work that found five CO ligands coordinated to UO_2^+.[30]

EXPERIMENTAL AND COMPUTATIONAL METHODS

Laser-ablated U atoms were reacted with N_2 in excess argon, neon, or nitrogen during condensation at 4 K using methods described in our previous papers.[11,31−34] The Nd:YAG laser fundamental (1064 nm, 10 Hz repetition rate with 10 ns pulse width) was focused onto a rotating uranium metal target (Oak Ridge National Laboratory, high purity, depleted of ^{235}U). The uranium target was filed to remove the oxide coating and immediately placed in the vacuum chamber. Isotopically scrambled molecular nitrogen was prepared by Tesla coil discharge of $^{14}N_2$ and $^{15}N_2$ (Cambridge Isotope Laboratories, 98+%) for 20 min at a pressure of 10−15 Torr in a Pyrex bulb with a stainless steel valve.

In the case of pure nitrogen, a mixture of $^{14}N_2$ and $^{15}N_2$ was passed through a 6 mm o.d. quartz tube with the orifice necked down to 1−2 mm and subjected to microwave discharge during deposition. This configuration worked best when the discharge glow extended out of the tube orifice like water from a garden hose. Mixtures of N_2 (0.5%) in argon were also subjected to microwave discharge excitation during codeposition with laser-ablated U atoms for spectroscopic examination. Then FTIR spectra were recorded at 0.5 cm^{-1} resolution on a Nicolet 750 spectrometer with an accuracy of 0.1 cm^{-1} using a HgCdTe range B detector. Samples were alternatively subjected to glass filtered Hg arc street lamp irradiation (Philips, 175 W) and temperature-cycled (i.e., annealed), as measured on a Au−Co versus Cu thermocouple embedded in the second-stage Sumitomo Heavy Industries RDK 205D cryocooler heat station flange supporting the OFHC copper mount for the CsI window. A radiation shield bolted to the first stage covered all but 0.5 in. diameter openings on each side to pass the IR beam.

Quantum-chemical calculations were done as performed previously with the hybrid B3LYP and pure BPW91 density functionals, the 6-311+G(3df) basis set for N, and the SDD pseudopotential [30 electron core] and optimized (12s11p10d8f) [8s7p6d4f] Gaussian valence basis set for U using the Gaussian 09 program system.[35−40] Additional PBE/def-TZVP and B3LYP/6-311+G(2df,p) DFT calculations and wave-function-based calculations using CASSCF/CASPT2 and the ANO-RCC-VTZP basis set were done in order to describe the multiconfigurational nature of UN and its complexes using methods described previously with the MOLCAS software.[17,41−43]

RESULTS AND DISCUSSION

Infrared spectra of the products of reactions of laser-ablated uranium atoms with dinitrogen in argon, nitrogen, and neon matrices will be presented, and the new dinitrogen complex assignments will be supported by quantum-chemical calculations. In addition, $U(NN)_x$ complexes will be presented and compared with those formed with UN and NUN.

Argon Matrix Spectra: $NUN(NN)_x$ Complexes. Infrared spectra of the products of reactions of laser-ablated uranium atoms with $^{14}N_2$, $^{15}N_2$, and $^{14,15}N_2$ (0.1, 0.5, and 2.5%) samples in excess argon during condensation at 4 K were recorded (Figures 1−4), and the important absorptions are listed in Table 1. Additional figures showing results for 10% $^{14}N_2$ in argon, 8% $^{15}N_2$ in argon, and pure nitrogen are given in Figures S1−S4 in the Supporting Information. These samples had minimum UO and UO_2 contaminants.[15,32]

The strong $U^{14}N_2$ and $U^{15}N_2$ bands at 1050.9 and 1019.4 cm^{-1} in solid argon exhibit an observed (anharmonic) $^{14}N/^{15}N$ frequency ratio of 1.03090, which is slightly lower than the calculated harmonic ratio 1.03117 (see the bold frequencies in Table 4). These strong absorptions are produced upon direct insertion of laser-excited U atoms into dinitrogen (eq 1), which is also initiated by full mercury arc (>220 nm) irradiation.[11,18] The reaction with $^{14}N^{15}N$ produces a strong 1040.7 cm^{-1} absorption for the antisymmetric stretching mode and a weak 987.2 cm^{-1} band for the symmetric stretching mode of $^{14}NU^{15}N$ (Figure 3), which demonstrates that this major product molecule contains two equivalent N atoms. The insertion reaction shown in eq 1 is exothermic by 57 kcal/mol at the B3LYP level or 69.8 kcal/mol at the CASPT2 level for ground-state U in the absence of spin−orbit coupling (SOC), which decreases to 48.8 kcal/mol when SOC is included,[18] but electronic excitation of U (either in the laser ablation process or through mercury arc irradiation in the

dx.doi.org/10.1021/jp501637j | J. Phys. Chem. A 2014, 118, 5289−5303

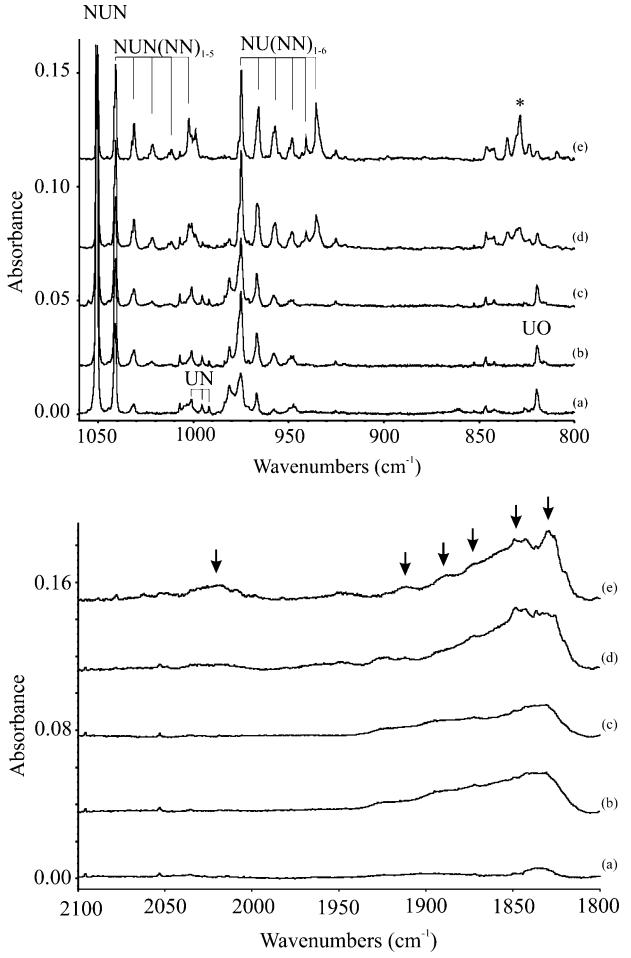

Figure 1. Infrared spectra of the major laser-ablated uranium + nitrogen reaction products upon codeposition in argon at 4 K. (a) U and $^{14}N_2$ (0.5%) codeposited in argon for 60 min, (b) after annealing to 30 K, (c) after >220 nm irradiation for 20 min, (d) after annealing to 35 K, and (e) after annealing to 45 K. The * label denotes a band that appears upon annealing and is probably due to a product that contains more than one U atom.

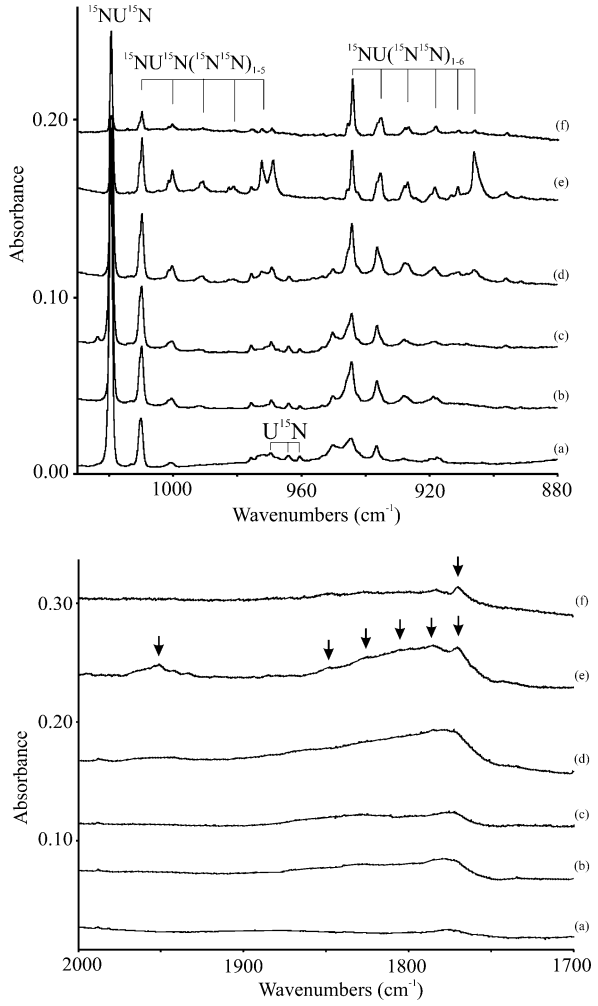

Figure 2. Infrared spectra of the major laser-ablated uranium + nitrogen reaction products upon codeposition in argon at 4 K. (a) U and $^{15}N_2$ (0.5%) codeposited in argon for 60 min, (b) after annealing to 30 K, (c) after >220 nm irradiation for 20 min, (d) after annealing to 35 K, and (e) after annealing to 45 K. (f) U and $^{15}N_2$ (0.1%) codeposited in excess argon at 5 K for 60 min and annealed to 45 K.

220−300 nm region) is required to activate this U* insertion reaction with the normally unreactive N_2 molecule.

$$\mathrm{U^* + N_2 \rightarrow NUN} \qquad \begin{aligned} \Delta E_{\mathrm{B3LYP}} &= -57.0\ \mathrm{kcal/mol} \\ \Delta E_{\mathrm{CASPT2}} &= -69.8\ \mathrm{kcal/mol} \\ \Delta E_{\mathrm{SOC}} &= -48.8\ \mathrm{kcal/mol} \end{aligned} \qquad (1)$$

Another isomer is formed upon an association reaction (eq 2), namely, UNN, which is 53.7 kcal/mol higher in energy at the B3LYP level in the quintet ground state than singlet NUN and has calculated stretching frequencies (intensities) of 1978 cm^{-1} (719 km/mol) and 265 cm^{-1} (4 km/mol). The triplet state is 6 kcal/mol higher in energy than quintet UNN. This molecule is observed here through a weak band at 1841 cm^{-1} in solid nitrogen, where higher-temperature annealing increases this absorption *without* activation energy and leads to more stable higher $U(NN)_x$ complex products.

$$\mathrm{U + N_2 \rightarrow UNN} \qquad \begin{aligned} \Delta E_{\mathrm{B3LYP}} &= -3.3\ \mathrm{kcal/mol} \\ \Delta E_{\mathrm{CASPT2}} &= -3.5\ \mathrm{kcal/mol} \end{aligned} \qquad (2)$$

In support of this conclusion, a very strong, broad 2098 cm^{-1} absorption with a major sideband at 2084 cm^{-1} for a red-shifted N−N stretching fundamental is observed in solid nitrogen with laser-ablated U atoms present (Figure 5 and Figure S4 in the Supporting Information), and it decreases upon UV irradiation to yield the $NUN(NN)_5$ complex in solid nitrogen, which will be discussed later. This suggests that $U(NN)_x$ complexes form when the N−N stretching fundamental is activated. A weak band is observed at 2079 cm^{-1} upon annealing to 35 K in our 10% N_2 argon matrix experiment, and it increases slightly upon further annealing to 40 and 45 K and then disappears upon annealing to 50 K. This band is probably due to the same species.

Upon matrix annealing, NUN molecules weakly interacting with dinitrogen molecules produce four decreasing-intensity satellite absorptions at 1041.0, 1031.4, 1021.6, and 1011.7 cm^{-1} (Table 1), but while these four bands increase, another band at 1002.6 cm^{-1} increases relatively much more. The first two of these were assigned in our first report on U + N_2 reactions to the $UN_2(N_2)_{1,2}$ complexes.[11] On the basis of our previous investigations with the isoelectronic CUO molecule and noble gas atoms,[26−29] there are at least four equatorial sites around the linear NUN molecule where Ar matrix atoms can be replaced by

dx.doi.org/10.1021/jp501637j | J. Phys. Chem. A 2014, 118, 5289−5303

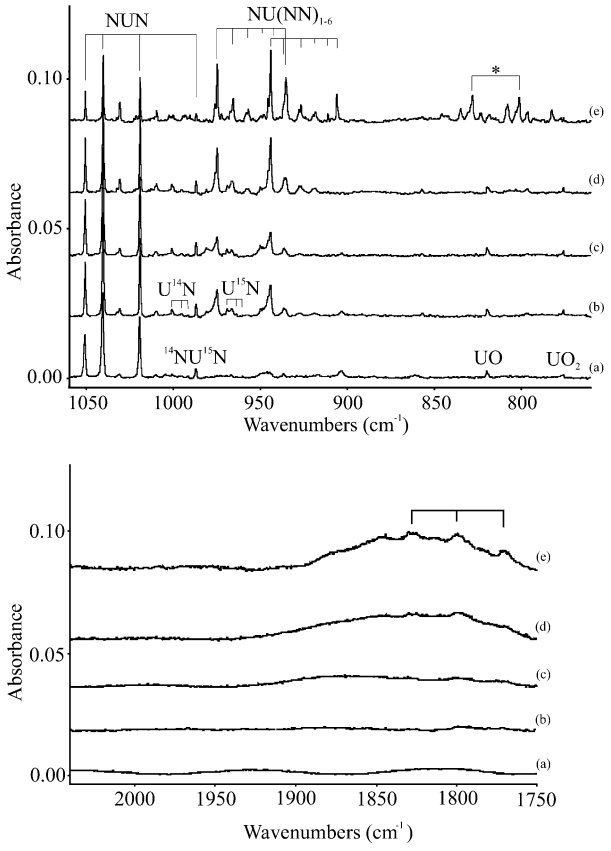

Figure 3. Infrared spectra of the major laser-ablated uranium + nitrogen reaction products upon codeposition in argon at 4 K. (a) U and $^{14}N_2/^{14}N^{15}N/^{15}N_2$ (0.1%) codeposited in argon for 60 min, (b) after annealing to 30 K, (c) after >220 nm irradiation for 20 min, (d) after annealing to 35 K, and (e) after annealing to 45 K. The * label denotes bands that appear upon annealing and are probably due to a product that contains more than one U atom.

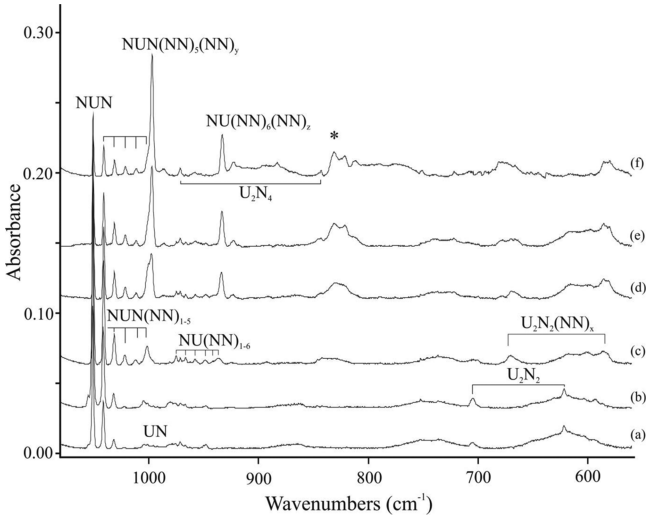

Figure 4. Infrared spectra of the major laser-ablated uranium + nitrogen reaction products upon codeposition in argon at 4 K. (a) U and $^{14}N_2$ (2.5%) codeposited in argon for 60 min, (b) after >220 nm irradiation for 20 min, (c) after annealing to 20 K, (d) after annealing to 30 K, (e) after annealing to 35 K, and (f) after annealing to 40 K. The * label denotes a band due to a diuranium species on the basis of annealing and concentration behavior.

N_2 molecules, Thus, these four bands at 1041.0, 1031.4, 1021.6, and 1011.7 cm^{-1} are assigned to the $UN_2(Ar)_x(N_2)_{1,2,3,4}$ complexes following our earlier work [henceforth, we will use the $NUN(NN)_x$ notation].[11] These bands all have $^{14}N/^{15}N$ isotopic frequency ratios near 1.03090, which is characteristic of the antisymmetric stretching mode of a linear N−U−N linkage. Of course, these complexes are surrounded by a secondary layer of argon atoms, as will become clearer on comparison with the neon and nitrogen matrix spectra. However, the possibility that five NN molecules might coordinate to the U center in NUN was brought to light by Duncan and co-workers, who found five CO ligands coordinated to UO_2^+.[30] The band at 1002.6 cm^{-1}, which increases upon annealing out of proportion to the 1041.0, 1031.4, 1021.6, and 1011.7 cm^{-1} band system, also exhibits the 1.03106 $^{14}N/^{15}N$ isotopic ratio for the core NUN mode, and it is probably due to a higher $NUN(NN)_x$ complex as well. It may be the case that the 1002.6 cm^{-1} band represents the upper limit of primary NN coordination with the U center. In pure solid nitrogen, the NUN absorption with N_2 molecules in both primary and secondary coordination roles is a very sharp absorption at 995.7 cm^{-1}.[12]

We performed a 2.5% N_2 experiment to help bridge the gap between the argon and nitrogen matrix environments, and the spectra are shown in Figure 4. The spectra are similar to those in Figure 1 in the 1050−1010 cm^{-1} region; however, the satellite absorptions were stronger relative to the 1050.9 cm^{-1} NUN band. Annealing to 20 K produced a new 1001.6 cm^{-1} band to terminate the satellite progression, which shifted to 997.7, 997.2, and 997.0 cm^{-1} upon successive higher-temperature annealing operations and dominated after the final annealing to 40 K (Figure 4f). Increasing the N_2 reagent concentration to 10% red-shifted the major bands slightly (measured after full arc irradiation) except for the last weak band in the progression (1050.0 to 1002.8 cm^{-1}; Table 3) and changed the relative band intensities markedly, as shown in Figure S1 in the Supporting Information. This confirms that the NUN vibrational progressions in the 1050−1000 cm^{-1} region are due to increasing numbers of NN ligands. However, annealing to 20 K changed the relative intensities and markedly *increased* the lowest-wavenumber band and red-shifted it from 1002.8 to 1001.3 cm^{-1}, while the five highest-wavenumber bands were increased slightly. The next annealing to 30 K broadened this feature and shifted it to 999.6−996.5 cm^{-1}, and then annealing to 35 K increased and sharpened this band to 995.4 cm^{-1}. The final annealings to 40 and 45 K increased this band even more at the expense of the higher-frequency features and sharpened and shifted it to 995.0 cm^{-1} (Figure S1g). This is almost the same frequency as the sharp 995.7 cm^{-1} band for NUN in pure solid nitrogen,[12] but the band in the argon matrix is an order of magnitude broader. Similar behavior was found for 8% $^{15}N_2$ in argon (Figure S3 in the Supporting Information), and these lower-wavenumber bands are also given in Table 3. They exhibit $^{14}N/^{15}N$ isotopic frequency ratios similar to those in the 0.5% reagent experiments (Figures 1 and 2). Accordingly, the above satellite bands are assigned to $NUN(NN)_{1,2,3,4,5}$ complexes, which are progressively more stable with higher complexation and terminate on the fifth satellite band at 1002.6 cm^{-1} using 0.5% N_2 reagent.

Several experiments were performed in which the Ar/N_2 reagent stream (0.5 and 2% N_2) was subjected to microwave discharge for codeposition with laser-ablated uranium. The product spectrum was similar to those reported above; however the 1051 cm^{-1} band was twice as strong and the 621.7 cm^{-1} band

dx.doi.org/10.1021/jp501637j | J. Phys. Chem. A 2014, 118, 5289−5303

Table 1. Observed Frequencies (cm^{-1}) for Uranium + Nitrogen Reaction Products in Solid Argon Using 0.5% N_2 and in Solid Nitrogen[a]

$^{14}N_2$	$^{14}N_2/^{14}N^{15}N/^{14}N_2$	$^{15}N_2$	$^{14}N/^{15}N$ freq. ratio	identification
		Absorptions in Solid Argon Using 0.5% N_2		
2020		1952	1.0348	$UN(NN)_x$
1950		1885	1.0345	$UN(NN)_x$
1912		1849	1.0341	UN(NN) isomer
1890		1827	1.0345	UN(NN) isomer
1873		1810	1.0348	UN(NN) isomer
1849		1787	1.0350	UN(NN) isomer
1830	1800	1770	1.0339	UN(NN)
1050.9	1040.7, 987.2	1019.4	1.03090	$NUN(Ar)_x$
1041.0	1031.1	1009.8	1.03090	$NUN(Ar)_4(NN)$
1031.4		1000.4	1.03099	$NUN(Ar)_3(NN)_2$
1021.6		990.8	1.03109	$NUN(Ar)_2(NN)_3$
1011.7		981.3	1.03098	$NUN(Ar)(NN)_4$
1002.6		972.4	1.03106	$NUN(NN)_5[Ar]_x\{Ar\}_y$
999.0		968.9	1.03107	$NUN(NN)_5[Ar,NN]_x\{Ar\}_y$
1007.4		975.7	1.03249	UN complex site
1001.1	1001.1, 969.5	969.5	1.03259	$UN(Ar)_6$
995.6	995.6, 964.1	964.1	1.03267	$UN(Ar)_5$
991.9	991.9, 960.6	960.6	1.03258	$UN(Ar)_4$
981.3		950.0	1.03295	$UN(NN)(Ar)_x$ site
975.1		944.2	1.03273	$UN(NN)(Ar)_5$
965.9		935.3	1.03272	$UN(NN)_2(Ar)_4$
957.1		926.7	1.03280	$UN(NN)_3(Ar)_3$
948.3		918.4	1.03256	$UN(NN)_4(Ar)_2$
940.9		911.1	1.03271	$UN(NN)_5(Ar)_1$
935.6		906.0	1.03267	$UN(NN)_6Ar_y$
925.3		896.2	1.03247	$UN(NN)_6[NN]_xAr_y$
835.0	*835.0, 808.0*	807.9	1.03354	U_xN
828.2	*828.5, 801.2*	801.2	1.03394	U_xN
705.5		683.5	1.03219	U_2N_2
704.3		682.3	1.03224	U_2N_2 site
699.7	*699.7, 677.3*	677.3	1.03307	U_xN_y
621.7	610	602.1	1.0326	$(U_2)N$
593.0	584	574.4	1.0324	U_2N_2
515.0		498.5	1.0331	U_xN_y
500.7		484.5	1.0334	U_xN_y
482.4	475, 468	466.8	1.0334	U_xN_y
		Absorptions in Pure Solid Nitrogen		
2328.0	2289.3	2250.0	1.0347	N_2
2098	broad	2029	1.0340	$U(NN)_7$
2083	featureless	2014	1.034	$U(NN)_7$
2070 sh		2002 sh	1.034	$U(NN)_7$
2043		1976	1.034	$U(NN)_7$
2021		1954	1.034	$U(NN)_7$
1841		1779	1.035	U(NN)
1785	1758	1731	1.0312	$U_2N_4(NN)_y$
1010.3		979.8	1.03113	$NUN(NN)_4[NN]_z$
995.7		965.6	1.03117	$NUN(NN)_5[NN]_z$
890.5		862.5	1.03246	$NU(NN)_5[NN]_z$
878.2		850.4	1.03269	$NU(NN)_6[NN]_z$
968.0		937.5	1.03253	$U_2N_4(NN)_y$
843.8	843.7, 831.8, 817.2	816.9	1.03293	$U_2N_4(NN)_y$
669.4	659.8	648.1	1.03287	$(UN)_2(NN)_x$ (ref 12)
580.2	569.8	561.7	1.03294	$(UN)_2(NN)_x$ (ref 12)
461.0	456.4	446.8	1.0318	$U_2N_4(NN)_y$

[a]Frequencies in cm^{-1}. Only new frequencies are listed for $^{14}N^{15}N$ reaction products. Bands that appear upon annealing are set in italic type.

was three times as strong, clearly dominating the 705.5 and 593.0 cm^{-1} absorptions, which are listed in Table 1.

The NUN complex with six NN ligands is not formed, and this complex is less stable, as shown by the approximate

dx.doi.org/10.1021/jp501637j | J. Phys. Chem. A 2014, 118, 5289−5303

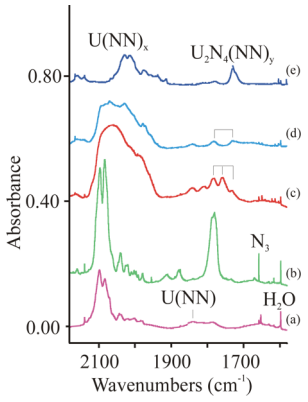

Figure 5. Infrared spectra of the N−N stretching region for products of the laser-ablated uranium and nitrogen reaction upon codeposition in pure nitrogen isotopic gases at 4 K. (a) U and $^{14}N_2$ codeposited for 30 min with a low-power microwave discharge of the depositing nitrogen sample, (b) U and $^{14}N_2$ codeposited for 60 min with a higher-power microwave discharge, (c) U and a 50/50 $^{14}N_2/^{15}N_2$ mixture codeposited with a higher-power discharge, (d) U and a 50/50 $^{14}N_2/^{15}N_2$ mixture codeposited with no discharge, and (e) U and $^{15}N_2$ codeposited with a higher-power discharge.

[B3LYP/6-311+G(2df,p)/SDD] reaction energies computed without correction for SOC, which should be small since UN_2 appears on both sides of these reactions (eqs 3). The lower $NUN(NN)_x$ complexes give way to the higher ones upon annealing, and the terminal band for $NUN(NN)_5$ increases at the expense of NUN and the $NUN(NN)_{1-4}$ complex absorptions, as shown in the figures. Calculated frequencies for the $NUN(NN)_{1,2,3,4,5}$ complexes are given in Table 4. It should be noted that the separation between the strong NUN fundamental and the $NUN(NN)_{1,2,3,4,5}$ complex absorptions is calculated as 18−20 cm^{-1} and that the observed separations are 9−10 cm^{-1}. The N−N stretching frequencies are computed to be red-shifted only a few reciprocal centimeters from the isolated NN molecular value and to have very low intensities (B3LYP), and these bands are too weak to be observed. The BPW91 functional clearly overestimates the intensities of these bands. It should also be noticed in Figure 7 that the N_2U-NN distance decreases from 2.83 to 2.81 Å in the range of stable complexes with one to five dinitrogen ligands, but it jumps up to 2.93 Å for the unstable complex with six dinitrogen ligands in the equatorial plane.

$$\begin{aligned}
UN_2 + N_2 &\rightarrow UN_2(NN) && \Delta E = -4.4\ \text{kcal/mol}\\
UN_2 + 2N_2 &\rightarrow UN_2(NN)_2 && \Delta E = -8.9\ \text{kcal/mol}\\
UN_2 + 3N_2 &\rightarrow UN_2(NN)_3 && \Delta E = -13.1\ \text{kcal/mol}\\
UN_2 + 4N_2 &\rightarrow UN_2(NN)_4 && \Delta E = -16.8\ \text{kcal/mol}\\
UN_2 + 5N_2 &\rightarrow UN_2(NN)_5 && \Delta E = -20.5\ \text{kcal/mol}\\
UN_2 + 6N_2 &\rightarrow UN_2(NN)_6 && \Delta E = -18.9\ \text{kcal/mol}\\
N_2 + UN_2(NN)_5 &\rightarrow UN_2(NN)_6 && \Delta E = +1.6\ \text{kcal/mol}
\end{aligned} \quad (3)$$

It is interesting to note that the principal NUN antisymmetric vibration for the supercomplex $NUN(NN)_5[NN]_xM_y$ (in this notation, the primary coordination layer is shown in parentheses, the secondary coordination layer is shown in square brackets, and the residual matrix shell is designated as M_y) changes from 1000.3 cm^{-1} for residual neon to 997.0 cm^{-1} for residual argon (with 2.5% N_2), to 995.7 cm^{-1} for pure nitrogen (see Tables 1−3).

Viswanathan and co-workers laser-ablated UO_2 into argon doped with N_2 and observed new bands at 984 and 974 cm^{-1} with 1% N_2; at 974, 964, 956, 948, and 940 cm^{-1} along with a broad feature at 797 cm^{-1} using 12% N_2; and sharper 938 and 796 cm^{-1} bands that tracked together using 50% N_2.[15] The 984 cm^{-1} band agrees with our earlier assignment to NUO,[13] and the five bands at 974, 964, 956, 948, and 940 cm^{-1}, which lead to the 938 cm^{-1} band for NUO in solid nitrogen, are appropriate for the five $NUO(NN)_{1,2,3,4,5}$ complexes following our above assignments to the five $NUN(NN)_{1,2,3,4,5}$ complexes.

Argon Matrix Spectra: $UN(NN)_x$ Complexes. Sharp, weak additional bands are observed at 1001.1, 995.6, and 991.9 cm^{-1} for $^{14}N_2$ and at 969.5, 964.0, and 960.6 cm^{-1} for $^{15}N_2$, which are precisely the bands first assigned to ^{14}UN and ^{15}UN, respectively, produced by codeposition of nitrogen discharged through uranium in excess argon by Green and Reedy.[10] Since these bands increase slightly upon annealing, it must be presumed that N atoms are produced from N_2 by high-energy radiation from the laser ablation plume and that the combination reaction shown in eq 4, which is the same reaction as performed earlier,[10] proceeds upon annealing, with an energy change of −147 kcal/mol (B3LYP). It is possible that the reaction of U* and N_2 could produce UN and N if the 78 kcal/mol of excess energy needed to break the NN triple bond in favor of the weaker UN triple bond is provided through U* excitation in the laser ablation process or irradiation in the ultraviolet region.

$$\begin{aligned}
&&\Delta E_{\text{B3LYP}} &= -147\ \text{kcal/mol}\\
U + N \rightarrow UN &&\Delta E_{\text{CASPT2}} &= -121.8\ \text{kcal/mol}\\
&&\Delta E_{\text{SOC}} &= -119.7\ \text{kcal/mol}
\end{aligned} \quad (4)$$

Diagnostic spectra from the 0.1% $^{14,15}N_2$ reaction are presented in Figure 3. The strong antisymmetric stretching and weak symmetric stretching absorptions for $^{14}NU^{15}N$ are noted at 1040.7 and 987.2 cm^{-1}, which reaffirm that this molecule contains two equivalent N atoms.[10−12] This stretching mode separation, 53.5 cm^{-1}, is slightly higher than the median of the values calculated for $^{14}NU^{14}N$ and $^{15}NU^{15}N$, namely, 40 cm^{-1} (Table 4). Furthermore, the $^{14}N/^{15}N$ isotopic frequency ratio of 1.03090 is characteristic of the antisymmetric stretching mode of a linear N−U−N linkage. The lack of any intermediate component in the UN isotopic spectra and the 1.0326 $^{14}N/^{15}N$ isotopic frequency ratio confirm the UN diatomic molecule character and assignment.[10]

The new band system at 975.1, 965.9, 957.1, 948.3, 940.9, and 935.6 cm^{-1}, which increases on annealing, is assigned to the $UN(N_2)_{1,2,3,4,5,6}(Ar)_x$ complexes. The most important characteristic of these bands is their diatomic UN $^{14}N/^{15}N$ isotopic frequency ratio (Table 1), which characterizes diatomic U−N vibrations as supported by the lack of intermediate isotopic components (Figure 3). It should be noted that six bands appear in this progression for UN complexes although only five appeared for the analogous NUN complexes. The sixth band, at 935.6 cm^{-1}, which increases much more than the five-band progression upon annealing, also has the UN diatomic ratio and no mixed isotopic component. This band appears to be the UN counterpart of the 1002.6 cm^{-1} NUN band and is likely to be due to a highest UN complex also involving five equatorial NN ligands in addition to the single axial NN ligand attached to the U center of the UN host molecule. Comparison of the 2.5% N_2 spectra in Figure 4 shows how this sixth terminal band, now at 933.8 cm^{-1}, dominates the UN-complex progression upon

dx.doi.org/10.1021/jp501637j | J. Phys. Chem. A 2014, 118, 5289−5303

successive annealing cycles. (The U_2N_2 bands follow the assignments in solid nitrogen by Kushto et al.[12]) With 10% N_2 we observe only three weak UN complex bands shifted to 971.4, 963.6, and 949.5 cm^{-1} upon deposition, which are replaced by the red-shifted terminal band at 932.4 cm^{-1} upon annealing (Figure S1 in the Supporting Information). It is important to note that UN absorbs even lower at 890.5 and 878.2 cm^{-1} in solid nitrogen (Figure S4 in the Supporting Information). This demonstrates the effect of the secondary coordination shell on the quartet UN core molecule complexes. Finally, we note that similar but less extensive $NW(NN)_x$ complexes were observed in the tungsten experiments.[25]

The weak band at 925.3 cm^{-1} after the sixth complex band in Figure 1A exhibits the diatomic UN $^{14}N/^{15}N$ isotopic frequency ratio, and it shifts to 923.1, 921.8, and 920.6 cm^{-1} as the nitrogen concentration is increased to 2.5, 10, and 100%. This feature likely occurs as a result of the $UN(NN)_6$ complex acquiring NN ligands in the secondary coordination shell.

The $UN(NN)_{1,2,3,4,5,6}$ complexes are progressively more stable with coordination of additional ligands, as given by our approximate (B3LYP) reaction energies, but the higher $UN(NN)_7$ complex is unstable toward NN elimination on the basis of the endothermic addition of NN to $UN(NN)_6$ (eq 5).

$$\begin{aligned}
&UN + NN \rightarrow UN(NN) && \Delta E = -22.6\ \text{kcal/mol}\\
&UN(NN) + NN \rightarrow UN(NN)_2 && \Delta E = -7.8\ \text{kcal/mol}\\
&UN(NN)_2 + NN \rightarrow UN(NN)_3 && \Delta E = -8.8\ \text{kcal/mol}\\
&UN(NN)_3 + NN \rightarrow UN(NN)_4 && \Delta E = -7.9\ \text{kcal/mol}\\
&UN(NN)_4 + NN \rightarrow UN(NN)_5 && \Delta E = -3.0\ \text{kcal/mol}\\
&UN(NN)_5 + NN \rightarrow UN(NN)_6 && \Delta E = -3.4\ \text{kcal/mol}\\
&UN(NN)_6 + NN \rightarrow UN(NN)_7 && \Delta E = +1.8\ \text{kcal/mol}
\end{aligned} \quad (5)$$

We attempted to calculate an Ar−UN complex using DFT and found a shallow minimum at a distance of 8 Å; thus, NN binds to UN much more strongly than does Ar. However, more argon atoms appear to interact more strongly as UN is stabilized in an argon matrix, with three "matrix site" absorptions at 1001.1, 995.6, and 991.9 cm^{-1}; the 1001.1 cm^{-1} band appears to be the most stable site, as our work shows that it is the dominant site. We suggest that these absorptions are due to the $NU(Ar)_{6,5,4}$ complexes, respectively.

There are striking differences between the NUN and UN dinitrogen complex systems. For NUN, the complex progression starts 9.9 cm^{-1} lower than isolated NUN and continues at intervals of 9.6, 9.8, 9.9, and 9.1 cm^{-1}, but for UN, the complex progression begins 16.8 cm^{-1} lower than the lowest UN matrix site and continues with intervals of 9.2, 8.8, 8.8, 7.4, and 5.3 cm^{-1}. Calculations using the PBE pure density functional, similar to those used successfully for many uranium-bearing systems,[25−29] explored doublet and quartet states for four different NU−NN structures (Table 5), and the bent quartet ($^4A''$) state was the lowest in energy. Additional calculations were done for this structure and state. It should be noted that the calculated separation between the UN and the $NU(NN)_x$ complex fundamentals is much larger than the interval between the NUN and the NN complexes, which agrees with experiment. Another difference between the NUN and UN complexes is the relatively larger intensity of the initial NUN band. Here we are dealing with the intense antisymmetric N−U−N stretching mode of a linear molecule relative to the U−N mode in a diatomic molecule. Moreover, the NN ligand interactions with the quartet-state UN center are much more complicated (particularly to compute) than for singlet NUN, and these binding energies are much stronger with UN (22.6 kcal/mol for the first NN ligand; eq 5) than with NUN (4.4 kcal/mol; eq 3).

The 1800−2100 cm^{-1} N−N stretching region contains new absorptions. First, a weak 1835 cm^{-1} band is observed upon deposition at 4 K, and this band and five absorptions marked by arrows increase on annealing, with the rightmost at 1830 cm^{-1} increasing more than the others upon later annealing. Weak 2020 and 1950 cm^{-1} bands also appear upon annealing. The set of bands beginning at 1830 cm^{-1} is probably due to NN interacting with UN. The calculated N−N fundamentals for the dinitrogen molecule in Table 4 for three methods B3LYP, BPW91, and CASPT2 are 116, 20, and 3 cm^{-1}, respectively, above the observed 2330 cm^{-1} fundamental value.[44] If the computed N−N frequencies for NU−NN are reduced by these amounts, N−N frequencies of 1843, 1821, and 2289 cm^{-1} are predicted, but only the former two are in good agreement with the observed 1830 cm^{-1} band system. The related bands at 1849, 1873, 1890, 1912 cm^{-1}, with approximately 20 cm^{-1} intervals, are most likely due to increasing packing arrangements of secondary layers of argon atoms around the NU−NN complex, but this must be considered tentative. A similar calibration and scaling for the strongest mode of the $UN(NN)_2$ complex predicts wavenumbers of 1965 and 1932 cm^{-1}, which are much higher than the above bands but appropriate for the weak 1950 cm^{-1} band. Likewise, a similar calculation predicts a wavenumber of 2047 cm^{-1} for the strongest absorption of $UN(NN)_3$, and the broad 2020 cm^{-1} absorption is in this region.

The NU−NN stretching mode is predicted to appear below 300 cm^{-1} with low intensity, which is lower than the range of our instrument. However, the structures in Figure 7 reveal interesting although slight changes in bond lengths. As the number of NN ligands increases, the U−N bond length increases from the UN value and the stretching frequency decreases; in addition, the U−NN bond length increases even more, while the N−N ligand bond length increases from the NN value. It is most important that the U−NN bond length increases dramatically for the unstable $NU(NN)_7$ complex!

Nitrogen Matrix Spectra. Laser-ablated U atoms were codeposited with pure nitrogen in our earlier investigation,[12] and more relevant details will be presented here. Figure 5 shows the N−N stretching region for different isotopic samples, deposition times, and microwave powers for the depositing nitrogen stream. A very strong band with structure at 2098, 2083, and 2070 cm^{-1} and weaker bands at 2043 and 2021 cm^{-1} were observed with natural isotopic material. These peaks shifted to 2029 and 2014 with $^{15}N_2$, and a clear intermediate component was observed at 2070 cm^{-1} with a mixture of $^{14}N_2$ and $^{15}N_2$. When a similar isotopic mixture was discharged into a statistical mixture, this band was broad and unstructured (Figure 5c). Two other features were observed at 1841 and 1785 cm^{-1} with $^{14}N_2$, where the latter increased markedly upon longer deposition with increased microwave discharge power and the former decreased. Only the 1841 cm^{-1} band was observed in this region with discharge of a 2% $^{14}N_2$ sample in argon. The former band shifted to 1779 cm^{-1} with $^{15}N_2$ and the latter one to 1731 cm^{-1}, giving isotopic frequency ratios of 1.0348 and 1.0312, respectively; however, the former exhibited no intermediate component when $^{14}N^{15}N$ was present while the latter had an intermediate band at 1758 cm^{-1}, as marked in Figure 5c. The N−N stretching region for these

dx.doi.org/10.1021/jp501637j | J. Phys. Chem. A 2014, 118, 5289−5303

samples is illustrated in Figure S4 in the Supporting Information, and it graphically demonstrates the effect of reacting laser-ablated U with a discharged nitrogen stream: the yields of uranium nitride species are increased substantially, but the $U(NN)_x$ complex species are little changed.

Expanded-scale spectra of samples formed by codepositing laser-ablated U atoms with discharged streams of $^{14}N_2$ and $^{15}N_2$ are illustrated in Figure S6 in the Supporting Information along with stick spectra calculated with the B3LYP functional for $U(NN)_7$ and scaled by the ratio of the strongest band observed at 2098 cm^{-1} and the strongest N−N stretching mode calculated at 2166 cm^{-1} (a factor of 0.969) . The six strongest N−N stretching modes are shown (the two calculated at 2115 and 2114 cm^{-1} are coincident in Figure S6), and all of the computed frequencies are given in the last table in the Supporting Information. The excellent agreement between the observed spectrum and that computed for $U(NN)_7$ provides strong support for the identification of this heptacoordinate complex, which follows from our previous identifications of the analogous $UN_2(N_2)_5$ and $NU(N_2)_6$ complexes, the gaseous $(CO)_5UO_2^+$ complex,[19] and numerous heptacoordinate ligand-supported cyanide complexes.[45,46]

The marked decrease in the $U(NN)_7$ complex in favor of the saturated $NUN(N_2)_5$ complex upon ultraviolet irradiation adds more evidence for a product of this stoichiometry, and its further growth upon annealing suggests strongly that the initial reaction shown in eq 2 to form U−NN is exothermic, as are subsequent additions of NN to the U center up to seven ligands; however, the addition of an eighth NN ligand is endothermic, as expected and summarized by the reactions shown in eq 6.

$$\mathrm{U} + 7\mathrm{NN} \rightarrow \mathrm{U(NN)_7} \quad \Delta E_{\mathrm{B3LYP}} = -72.5\ \mathrm{kcal/mol}; \quad \Delta E_{\mathrm{CASPT2}} = -80.1\ \mathrm{kcal/mol}$$

$$\mathrm{U(NN)_7} + \mathrm{NN} \rightarrow \mathrm{U(NN)_8} \quad \Delta E_{\mathrm{B3LYP}} = +3.1\ \mathrm{kcal/mol} \qquad (6)$$

Neon Matrix Spectra: $NUN(NN)_x$ and $(NN)_xUN$ Complexes. Laser-ablated uranium atom reaction products with $^{14}N_2$ and $^{15}N_2$ (0.05 and 0.2%) in excess neon during condensation at 4 K give the spectra shown in Figure 6 and Figure S5 in the Supporting Information, and the important new absorptions are listed in Table 2. Not shown are sharp absorptions at 2237.5 and 1815.8 cm^{-1}, which shift to 2163.1 and 1755.2 cm^{-1} upon $^{15}N_2$ substitution and disappear upon full arc irradiation. The former bands have been assigned to N_4^+ in solid neon,[47] and their observation here attests to the presence of photoionizing radiation in the uranium laser ablation plume.

The strong $U^{14}N_2$ and $U^{15}N_2$ bands at 1076.7 and 1044.4 cm^{-1} in solid neon reveal site splittings upon annealing, but these retain almost the same $^{14}N/^{15}N$ isotopic frequency ratio as the 1076.7 cm^{-1} band (1.03093) for the antisymmetric stretching mode of a linear N−U−N linkage. Four lower-frequency bands with weak structure give rise to sharp features at 1063.8, 1050.3, 1036.6, and 1021.9 cm^{-1} upon annealing, which define $^{14}N/^{15}N$ isotopic frequency ratios near 1.0309 (Table 2) that are again appropriate for the antisymmetric stretching mode of linear NUN, this time with 1−4 NN ligands, respectively. Two additional broader features are observed at 1010 and 1000 cm^{-1} upon annealing, and these also have $^{14}N/^{15}N$ isotopic frequency ratios characteristic of linear NUN. We suggest that these bands are due to $NUN(NN)_5$ complex species with different proportions of NN and Ne in the secondary coordination shell.

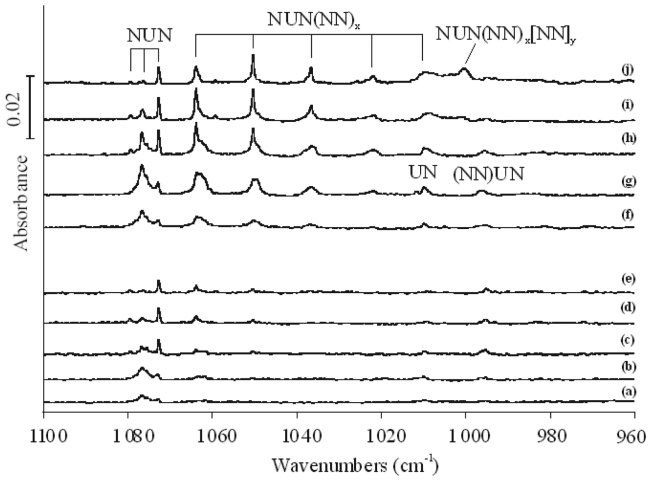

Figure 6. Infrared spectra of the major products of the reaction of laser-ablated uranium and nitrogen upon codeposition in neon at 4 K. (a) U and $^{14}N_2$ (0.05%) codeposited in neon for 40 min, (b) after >220 nm irradiation for 20 min, (c) after annealing to 8 K, (d) after annealing to 10 K, and (e) after annealing to 11 K. (f) U and $^{14}N_2$ (0.2%) codeposited in neon for 40 min, (g) after >220 nm irradiation for 20 min, (h) after annealing to 8 K, (i) after annealing to 10 K, and (j) after annealing to 11 K.

Table 2. Observed Frequencies (cm^{-1}) for Uranium + Nitrogen Reaction Products in Solid Neon

$^{14}N_2$	$^{15}N_2$	$^{14}N/^{15}N$ freq. ratio	identification
2237.5	2163.1	1.03440	N_4^+
1815.8	1755.2	1.03453	UN(NN)
1079.5	1047.0	1.03104	NUN site
1076.7	1044.4	1.03093	$NUN(Ne)_{sat}$
1072.7	1040.7	1.03075	NUN site
1063.8	1009.8	1.03081	$NUN(Ne)_4(NN)$
1050.3	1000.4	1.03102	$NUN(Ne)_3(NN)_2$
1036.6	990.8	1.03093	$NUN(Ne)_2(NN)_3$
1021.9	981.3	1.03108	$NUN(Ne)_1(NN)_4$
1011.7	979.8	1.03256	UN site
1009.9	977.8	1.03283	UN
996.2	964.7	1.03265	UN(NN)
	953.8		$UN(NN)_2$
1010 br	980 br	1.0306	$NUN(NN)_5[Ne_y]$
1000.3	970.1	1.03113	$NUN(NN)_5[NN]_xNe_y$
709.8			$(UN)_2$

An interesting comparison of the NUN and NN complex bands in solid argon and neon is displayed in Table 3. It should be noticed that the neon-to-argon matrix shift decreases from 26.8 to 10.2 to 7.4 cm^{-1} with increasing NN ligation and therefore with a decrease in the number of noble gas atoms left in the primary coordination sphere. This residual 7 cm^{-1} shift reflects the effect of the secondary noble gas coordination layer around the primary $NUN(NN)_5$ complex. Such a logical observation also supports our identification of the NUN dinitrogen−noble gas complexes.

Two additional weak bands are observed in solid neon, at 1009.9 and 996.2 cm^{-1}, and these bands have $^{14}N/^{15}N$ isotopic frequency ratios of 1.03283 and 1.03265, which signify diatomic U−N vibrations. These bands increase upon full arc irradiation and decrease upon further annealing. The sharp 1009.9 cm^{-1} band is assigned to the diatomic UN molecule in solid neon. The neon-to-argon matrix shift of 1009.9 − 1001.1 = 8.8 cm^{-1} is

dx.doi.org/10.1021/jp501637j | J. Phys. Chem. A 2014, 118, 5289−5303

Table 3. Comparison of Frequencies (cm^{-1}) for Uranium and N_2 Reaction Products in Solid Neon and Argon

neon (0.05% $^{14}N_2$)	argon (0.5% $^{14}N_2$)	Ne−Ar shift	argon (10% $^{14}N_2$)	argon (8% $^{15}N_2$)	$^{14}N/^{15}N$ freq. ratio	identification
1076.7	1050.9	26.8	1050.0	1019.1	1.0303	$NUN(Ng)_{saturated}$
1063.8	1041.0	22.8	1040.5	1009.9	1.0303	$NUN(Ng)_4(NN)$
1050.3	1031.4	18.9	1030.8	1000.6	1.0302	$NUN(Ng)_3(NN)_2$
1036.6	1021.6	17.0	1021.3	991.2	1.0304	$NUN(Ng)_2(NN)_3$
1021.9	1011.7	10.2	1011.6	981.5	1.0307	$NUN(Ng)_1(NN)_4$
1010.0	1002.6	7.4	1002.8	972.6	1.0310	$NUN(Ng)_0(NN)_5$
			999.6−996.5	969.2−966.6		$NUN(NN)_5[NN]_xAr_y$
			995.0	965.2	1.0309	$NUN(NN)_5[NN]_x$
1000.3						$NUN(NN)_5[NN]_xNe_y$
1009.9	995.6	14.3				$UN(Ng)_5$
996.2	975.1	21.1				$UN(Ng)_4(NN)$
n. o.	965.9					$UN(Ng)_3(NN)_2$
n. o.	957.1					$UN(Ng)_2(NN)_3$
n. o.	948.3					$UN(Ng)_1(NN)_4$
n. o.	940.9					$UN(Ng)_0(NN)_5$
	935.6		931.6			$UN(Ng)_0(NN)_6$

reasonable for this molecule with some polar bond character.[48] The 996.2 cm^{-1} band is appropriate for the first UN−NN complex in solid neon, and the ^{15}N counterpart of the $UN(NN)_2$ complex is found at 953.8 cm^{-1}.

Calculations on U, UN, and NUN Complexes with N_2. DFT calculations were first done for NUN complexes with N_2, since both NUN and NN have singlet ground states. N≡U≡N is a triple-bonded species with short U−N bond lengths computed as 1.73 Å at the CASPT2 level.[47] In contrast, tetravalent Th forms the linear dinitride N═Th═N with double bonds of length 1.876 Å (see Figure S7 in the Supporting Information), which absorbs at 756.6 cm^{-1} in solid argon.[12] In contrast, N═W═N in the triplet ground state is bent and has a longer bond length (Figure S7) and lower antisymmetric stretching frequency (878.3 cm^{-1}) than W≡N, which exhibits a 1059.5 cm^{-1} fundamental for the quartet ground state in solid argon,[25] about 60 cm^{-1} higher than that of U≡N. Although side-bound dinitrogen complexes with NUN did not converge, the end-bonded complexes shown in Figure 7 gave all real frequencies, and the NUN frequencies (Table 4) correlate well with the values observed in these matrix isolation experiments.

In order to explore the addition of NN to the UN center, calculations were done for NU−NN complexes in doublet and quartet states. A bent quartet was the lowest-energy state for NU−NN using the PBE functional (Table 5). The (9,16) active space was chosen for CASPT2 calculations on UN, as described previously;[49] at the CASPT2 level, $^4\Gamma$ was the ground state with $^4\Phi$ 3.4 kcal/mol higher, and the ground state had a converged bond length of 1.757 Å and a frequency (intensity) of 1034 cm^{-1} (275 km/mol). In contrast, thorium also forms a nitride, doublet ThN with a bond length of 1.805 Å and a frequency of 934.3 cm^{-1} in solid argon, but doublet ThN does not form the extensive series of NN complexes that quartet UN does.[12] Very recently, the gas-phase ground-state UN bond length has been measured as 1.7650(12) Å,[19] which is in excellent agreement with our CASPT2 value given above. An effective bond order (EBO) of 2.87 was obtained from the bonding and antibonding populations in the UN molecular orbitals (MOs) and the unpaired electrons in the 7s and 5f orbitals on U (Figure 9 top). However, the NU−NN complex was destabilized with this active space, presumably because NN MOs were not included. We found that a (13,13) active space including NN π orbitals and electrons gave a more reasonable orbital picture (Figure 9 bottom).

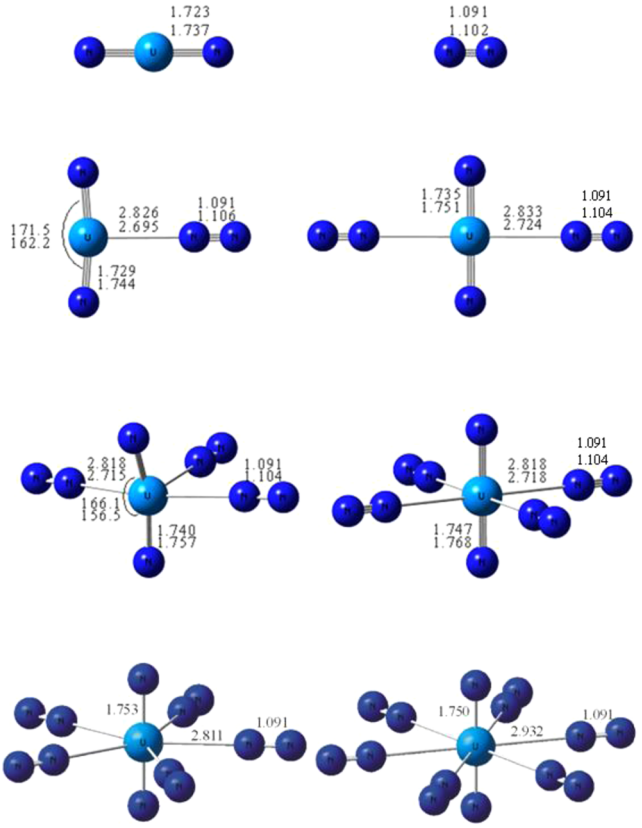

Figure 7. Optimized structures of NUN, NN, and $NUN(NN)_{1,2,3,4,5,6}$ complexes using the B3LYP (top and single numbers) and BPW91 (bottom numbers) density functionals.

Although the EBO for the UN subunit was not changed, the π EBO computed for the NN ligand was reduced from 1.88 to 1.86 in accord with the lower B3LYP frequency of 1954 cm^{-1} for the nitrogen ligand. Figures 7 and 8 compare the structures of the $NUN(NN)_{1-5}$ and $NU(NN)_{1-6}$ complexes, respectively.

The NUN molecule was described using the (12,13) active space, which gave a bond length of 1.733 Å, an antisymmetric harmonic frequency (intensity) of 1095 cm^{-1} (521 km/mol), and an EBO of 2.87 for the $^1\Sigma_g^+$ ground state.[49] The vibrational frequencies for these molecules have been observed only in solid matrices, and the calculated frequencies compare favorably with

dx.doi.org/10.1021/jp501637j | J. Phys. Chem. A 2014, 118, 5289−5303

Table 4. Calculated Highest of All Real Frequencies (ν, cm^{-1}), Infrared Intensities (I, km/mol), and Bond Lengths (d, Å) for UN, NUN, and Their NN Complexes[a]

	B3LYP	BPW91	CASPT2
^{4}X UN: ν (I), d	1037 (215), 1.751	1005 (179), 1.759	1034 (275), 1.757
$^1\Sigma_g^+$ NN: ν (I), d	2446 (0), 1.091	2350 (0), 1.102	2333 (0), 1.105
^{4}A″ NU−NN:			
ν (I)	1954 (2804), 989 (331), 261 (32)	1835 (1671), 973 (237), 292 (24)	2292 (6740), 1004 (327), 361 (197)
d_{N-U}, d_{U-N}, d_{N-N}	1.757, 2.357, 1.127	1.768, 2.286, 1.150	1.75, 2.23, 1.15
$\langle S^2 \rangle$	3.78	3.77	
$^1\Sigma_g^+$ NUN isotopologues: ν (I)			
^{14}NU^{14}N	**1111.7 (566), 1073.4 (0), 104.8 (102 × 2)**		
^{14}NU^{15}N	**1101.5 (486), 1048.7 (63), 103.3 (99 × 2)**		
^{15}NU^{15}N	**1078.1 (532), 1037.1 (0), 101.7 (96 × 2)**		
N−U−N: d, θ	1.723, 180°	1.737, 167°	1.733, 180°
NUN(NN)$_x$ complexes: ν (I)			
NUN	1116.8 (582)		
NUN(NN)	1098.7 (564)	1051.2 (423)	
	2442.9 (4)	2275.7 (214)	
NUN(NN)$_2$	1080.6 (550)	1029.8 (416)	
	2446.5 (5)	2304.8 (184)	
NUN(NN)$_3$	1062.5 (512)	1008.6 (334)	
	2441.8 (10)	2300.0 (224)	
NUN(NN)$_4$	1041.5 (506)	980.6 (341)	
	2441.3 (12)	2302.4 (201)	
NUN(NN)$_5$	1023.5 (476)		
	2440.2 (19 × 2)		
NUN(NN)$_6$	1030.5 (476)		
	2444.7 (11 × 2)		

[a]Dimensions for NUN(NN)$_x$ are given in Figure 7. B3LYP and BPW91 used 6-311+G(3df) and SDD basis sets with the Gaussian 09 program system. The bold set of NUN isotopic frequencies were computed with B3LYP and the def-TZVP/SDD basis set. Wave-function-based calculations were done using CASSCF/CASPT2, the (9,13) active space, and the ANO-RCC-VTZP basis set with MOLCAS; this gives a $^4\Gamma$ ground state for UN (see ref 49). A complete table of NU(NN)$_x$ frequencies is given in Table S1 in the Supporting Information.

Table 5. Optimized Geometries Computed for NU−NN Isomers with PBE/def-TZVP/SDD: Relative Energies (E_{rel}, kcal/mol), $\langle S^2 \rangle$ Values, Distances (Å), Frequencies (cm^{-1}), and Intensities (km/mol)

				distance		frequency (intensity)	
geometry	mult.	E_{rel}	$\langle S^2 \rangle$	N−U	N−N	N−U	N−N
linear	2	102.9	0.75	1.839	1.200	801 (76)	1628 (296)
	4	60.6	4.68	1.877	1.184	762 (184)	1665 (326)
bent	2	8.5	0.76	1.761	1.153	993 (221)	1853 (1436)
	4	0.0	3.77	1.768	1.151	983 (218)	1861 (1580)
side-on planar	2	12.6	0.75	1.766	1.656	863 (36)	952 (92)
	4	48.7	3.86	1.832	1.336	826 (87)	1114 (47)
side-on nonplanar	2	12.6	0.75	1.767	1.653	866 (34)	951 (93)
	4	30.0	3.75	1.823	1.357	841 (89)	1079 (38)

the matrix observations (UN, 1001 cm^{-1} in Ar and 1010 cm^{-1} in Ne; NUN, 1051 cm^{-1} in Ar and 1076 cm^{-1} in Ne),[10,11,31] as found with earlier calculations.[16,49]

Next, calculations were done for quartet UNN, first with B3LYP, and the linear form with a 1978 cm^{-1} (719 km/mol) N−N stretching mode was 17 kcal/mol lower than the side-bound isomer. The weak band at 1841 cm^{-1} in pure nitrogen shifts to 1799 cm^{-1} with an isotopic frequency ratio of 1.0348, corresponding to that for an N−N stretching vibration. Both mixed ^{14,15}N experiments show the 1841 cm^{-1} band, but the 1799 cm^{-1} counterpart is covered. A similar band appears at 1835 cm^{-1} upon sample deposition in solid argon (Figure 1, lower panel). These bands are appropriate for the UNN complex formed in the reaction shown in eq 2. In the pure nitrogen sample with U atoms present, UV irradiation increases the 1841 cm^{-1} band and the NUN(NN)$_x$ band system and decreases the very strong feature at 2098 and 2083 cm^{-1}. However, annealing at 20 K removes the weaker 1841 cm^{-1} band and restores much of the very strong band.

Following the sevenfold coordination of the U centers discussed above, we computed the structure of the U(NN)$_7$ complex and found it to be stable. Figure 10 compares its structure with those of the analogous complexes NUN(NN)$_5$ and NU(NN)$_6$ (from Figures 7 and 8, respectively), and the N−N stretching frequencies are given in the last table in the Supporting Information. Nearly all of the extremely high intensity of this absorption is concentrated in very strong modes computed at 2166, 2162, and 2150 cm^{-1} (5000 km/mol) and 2115, 2114, and 2095 cm^{-1} (2000 km/mol), which is a reasonable model for the broad observed feature at 2098 and 2083 cm^{-1} and weaker peaks

dx.doi.org/10.1021/jp501637j | J. Phys. Chem. A 2014, 118, 5289−5303

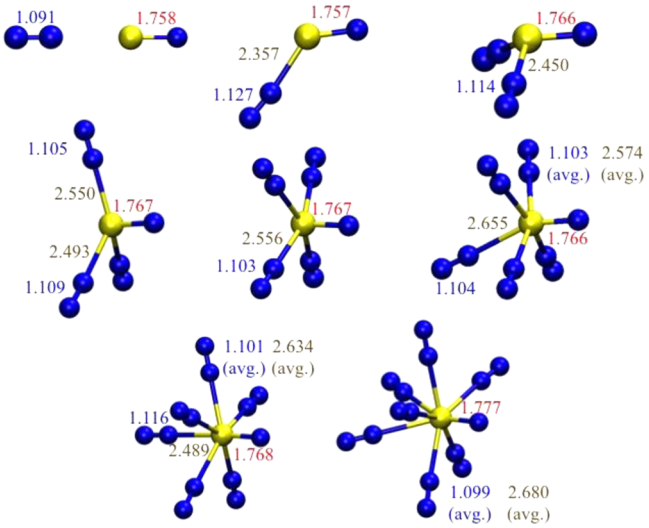

Figure 8. Structures of NN, UN, and NU(NN)$_{1-7}$ complexes calculated at the B3LYP/SDD/6-311+G(2df,p) level. Red numbers are U−N bond lengths, gold numbers are NN−UN bond lengths, and blue numbers are N−N bond lengths. The trends with increasing NN coordination should be noted.

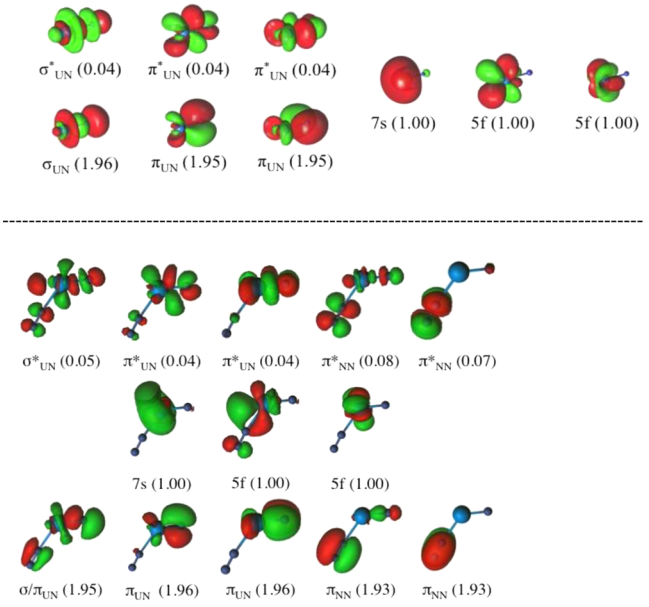

Figure 9. (top) Selected natural orbitals from the (9,16) active space of the UN molecule. Occupation numbers are given in parentheses. Only orbitals with occupation numbers larger than 0.01 are shown. (bottom) Selected natural orbitals from the (13,13) active space of the NU(NN) molecule. The net NN π bonding has been reduced to 3.71 electrons in the NU(NN) complex.

at 2070, 2043, and 2021 cm^{-1}. These bands shift upon $^{15}N_2$ substitution (Figure 5e) and give the isotopic frequency ratios of 1.0340 expected for pure N−N stretching modes. The experiment with mixed $^{14}N_2$ and $^{15}N_2$ revealed an intermediate peak, indicating that multiple NN molecules participate in this vibrational mode and complex.

In the U(NN)$_x$ series, for each additional nitrogen molecule that is coordinated to the uranium metal center, the U−N_2 interactions become weaker on average, and the nitrogen bonding orbitals mix with the metal center to a lesser extent. Since N_2 binding to U is relatively weak, a (6,13) active space on the uranium center and on the U(NN)$_x$ product was sufficient. The nitrogen molecule was treated at the MP2 level since no nitrogen orbitals are in the active space in the product. However, this assumption broke down for UNN. In this case, the computed reaction energy was nearly zero. In order for this species to be synthesized under the experimental conditions, the reaction energy must be negative. Therefore, CASPT2 calculations with a large active space (12 electrons in 19 orbitals) were performed. This space includes the 13 valence orbitals of uranium and also the nitrogen σ and π systems (see Figure 11). While the ground state of this molecule can be treated using this larger active space, in order to include corrections from spin−orbit coupling, low-lying excited states must also be computed, and this was computationally prohibitive. Therefore, restricted active space self-consistent field (RASSCF) calculations with corrections from second-order perturbation theory (RASPT2) were also employed. The total space remained (12,19), and the 13 orbitals corresponding to uranium remained in RAS2. The nitrogen σ and π orbitals were placed in RAS1 and the σ* and π* orbitals in RAS3. Two holes and two electrons were allowed in RAS1 and RAS3, respectively.

In order to quantify the binding energy of UNN, the change in energy for the reaction shown in eq 2 was computed. The standard approach is to compute the reactants individually, taking care to ensure that correlation is treated at the same level on both sides of the reaction (e.g., the active space must be consistent). To ensure this was the case, reactants were computed together separated by a distance of 100 Å. This approach also ruled out errors arising from basis set superposition error, as both the reactants and products included the same number of basis functions. With the large active spaces previously described, the computed changes in energy for the reaction were −1.1 and −3.8 kcal/mol at the CASPT2 and RASPT2 levels of theory, respectively. Ideally, we would have liked to include more excitations in the RASSCF calculation; however, these larger calculations (like the original CASSCF space) became computationally intractable when a state-averaged calculation including higher states was performed. Therefore, spin−orbit (SO) corrections were added a posteriori to the RASSCF space described above using the restricted-active-space state interaction (RASSI) approach. In this work, we followed the so-called SO-RASPT2 approach in which diagonal elements of the spin Hamiltonian computed at the RASSCF level of theory are replaced with RASPT2 energies for each state. The correction to the reactants was larger than that to the products, thereby reducing the change in energy from −3.8 kcal/mol to −0.7 kcal/mol. The small differences in energy highlight the inherent challenges in computing the thermochemistry for small actinide-containing systems. The ground state of UNN is highly multireference, with four electron configurations contributing ∼20% each to the total wave function while all other configurations contributed less than 0.1%.

Spin−orbit effects were included using the complete-active-space state interaction (CASSI) method or the analogous RASSI method, depending on which type of wave function calculation was performed. In this approach, an effective one-electron SO Hamiltonian based on the atomic mean-field approximation for the two-electron contributions is employed. The CASSCF calculations are performed for the spin states and symmetries of interest, and the resulting functions are used as basis functions in the SO Hamiltonian. The CASPT2 energies are taken as the diagonal elements of the Hamiltonian. When computing binding energies for CASSCF/CASPT2 calculations, it is essential to treat correlation at the same level of theory for the reactants and

dx.doi.org/10.1021/jp501637j | J. Phys. Chem. A 2014, 118, 5289−5303

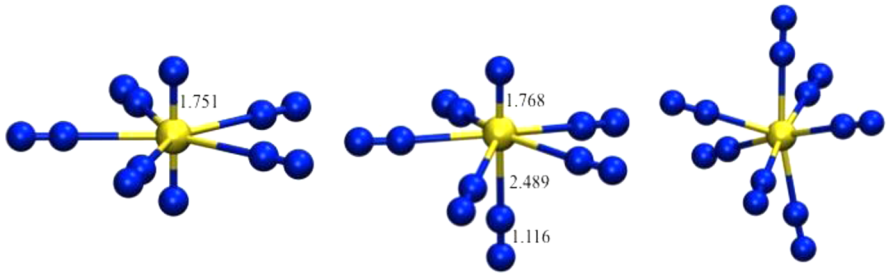

Figure 10. B3LYP-calculated structures of the three sevenfold-coordinated complexes observed here, all plotted on the same scale. The average U−N bond distances are 2.811, 2.634, and 2.491 Å.

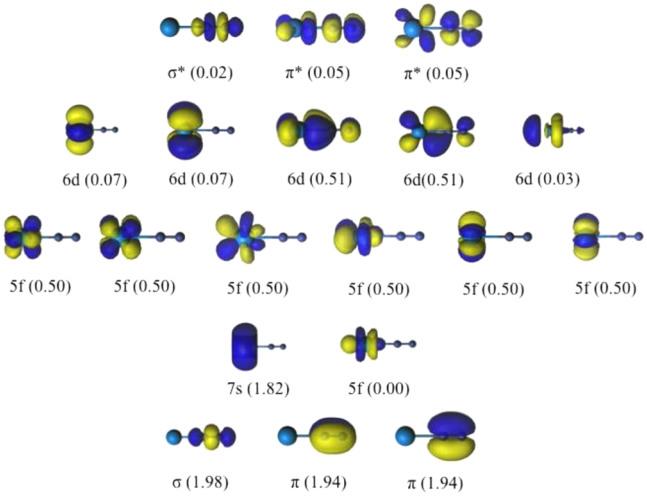

Figure 11. Active natural orbitals from the (12,19) CASSCF calculation on the ground state of UNN. The occupation numbers are given in parentheses.

the products. Moving to RASSCF can easily introduce errors since the number of excitations may not be the same even if the total numbers of active electrons and orbitals are the same for the reactants and products. Computing the reactants at 100 Å is analogous to computing a dissociation curve. By simply increasing the distance between A and B (in our case, A = U and B = N_2), we can ensure that the level of theory is exactly the same for the reactants and products. In this way we can ensure that the correlation treatment and basis sets are consistent on both sides of the reaction.[50]

Moreover, as additional N_2 groups are added stepwise (i.e., as x increases), the energy for the reaction in eq 2 becomes increasingly more negative. For x = 2, 3, and 7 the energies are −12.3, −28.6, and −72.5 kcal/mol, respectively. Furthermore, at the CASPT2 level of theory with a (6,13) active space, the reaction energy when x = 7 is −80.1 kcal/mol. Hence, we believe that $U(NN)_7$ is the final stable complex formed with U atoms in a pure nitrogen matrix. Clearly, its photodestruction leads to $NUN(NN)_5$ complexes.

One of our referees raised the question of comparing the populations of the far and near N atoms in U−NN, in view of the fact that uranium appears to prefer the isocyanide (U−NC) rather than the cyanide (U−CN) arrangement.[51,52] We performed a geometry optimization for the quartet ground state of the isocyanide UNC at the same B3LYP level of theory used in the present work for the UNN linear quintet. At the DFT geometry, a CASSCF/CASPT2 calculation was performed using a (5,13) active space. Above we discussed the need for a larger active space on UNN; however, this was necessary to compute the dissociation energy appropriately. The smaller active space was sufficient to compare the ground states of UNC and UNN. At the CASSCF level, the isocyanide has a Mulliken spin density of 2.99 on uranium while UNN has a spin density of 3.49, consistent with the difference in ground spin states. The coordinating N atoms have spin densities of 0.0016 and 0.2039 for UNC and UNN, respectively. Likewise, the spin density for the terminal C in UNC is 0.0031, while that for N in UNN is 0.3105. The atomic charges are $U^{0.55}-N^{-0.19}-N^{-0.36}$ and $U^{0.28}-N^{-0.14}-C^{-0.14}$. The lower charge on U in UNC is consistent with the difference in spin state between the two species (quartet for UNC and quintet for UNN). These differences can be reflected in the natural orbitals as well. In UNN, two 5f and two 6d orbitals hybridize and interact with the 2p N orbitals. In UNC this does not occur, and the 5f orbitals remain localized on the uranium center. This is nicely illustrated in the natural orbitals shown in Figure 12.

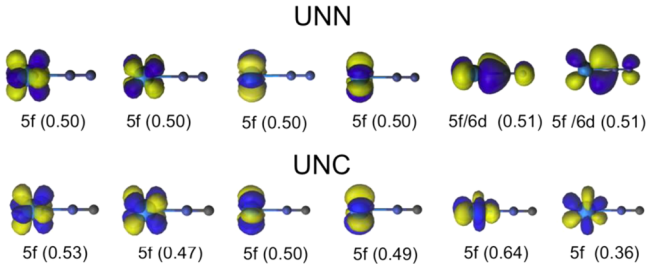

Figure 12. Selected natural orbitals from the (6,13) active space of UNN and the (5,13) active space of UNC.

Comparisons with Multicyclic-Ligand-Stabilized UN Complexes. How do the UN molecule and its $NU(NN)_{1-6}$ complexes prepared here compare with the multicyclic-ligand-stabilized terminal uranium(V) nitride complex with a terminal UN bond of length 1.825(15) Å and a 955 cm^{-1} stretching mode?[5] Both have nominal U≡N triple bonds, as CASPT2 calculations reveal an EBO of 2.87 for isolated UN and a DFT-computed Mayer bond order of 2.91 has been reported for the ligated complex.[6,7] However, isolated U≡N has a shorter calculated bond length of 1.757 Å (CASPT2) and a higher calculated frequency of 1034 cm^{-1} to go with higher observed frequencies of 1010 cm^{-1} in solid neon and 1001 cm^{-1} in solid argon. Another UN-bearing species, IrUN, which was found through calculations, has a terminal nitride length of 1.749 Å (CASPT2).[53] As a reference point, the gas-phase UN diatomic molecule bond distance has just been measured as 1.7650(12).[19] Of more importance for matrix-isolated UN is the observed $U^{14}N/U^{15}N$ isotopic frequency ratio of 1.0326, which is appropriate for an essentially pure U−N bond stretching vibration, and the smaller 955/930 = 1.0269 ratio for the cyclic ligand complex indicates considerable vibrational mode coupling with the ligating nitrogen

dx.doi.org/10.1021/jp501637j | J. Phys. Chem. A 2014, 118, 5289−5303

centers. Although six coordinating N_2 ligands reduce the U−N stretching frequency to 935 cm^{-1} in solid argon for the $N{\equiv}U(NN)_6$ complex, the terminal U≡N stretching mode is still a pure U−N mechanical vibration based on its $^{14}N/^{15}N$ isotopic ratio of 1.0327. It is clear that any ligand coordinating to the UN center, even simple NN, will affect the U−N bond length and the U−N vibrational frequency. Hence, the reference point must be to isolated UN itself, which has been observed only in solid argon, solid neon, and the gas phase.[10,13,16,19]

In fact, the simple U≡N triple bond was discovered first in matrix isolation investigations,[10−14] long before any bulk synthetic ligand work was reported, and U≡N was characterized at the CASPT2 level of theory in our earlier publication on $N{\equiv}UF_3$[17] and in work comparing U≡N with U≡P.[49] Nevertheless, in the same issue of *Science* in 2012 in which the above bulk synthesis[6] appeared, a paper entitled "Uncovering the Uranium−Nitrogen Triple Bond"[54] was published that celebrated the bulk synthesis without any mention of the matrix isolation work that resulted in the small-scale preparation of the terminal uranium nitrides U≡N and N≡U≡N from 1976, 1993, 1997, 1998, 1999, and 2011.[10−14,16]

CONCLUSIONS

New experimental and computational investigations of the products of reactions of laser-ablated U atoms with N_2 molecules upon codeposition in excess argon or neon at 4 K have revealed intense N≡U≡N and weak U≡N absorptions of complexes containing terminal uranium−nitrogen triple bonds. Annealing produced progressions of additional new absorptions for the $N{\equiv}U{\equiv}N(N_2)_{1,2,3,4,5}$ and $U{\equiv}N(N_2)_{1,2,3,4,5,6}$ complexes based on experiments with nitrogen concentrations from 0.1 to 10% and on nitrogen $^{14}N/^{15}N$ isotopic frequency ratios that are different for the UN and NUN modes characterized here. The neon-to-argon matrix shift of the N−U−N antisymmetric stretching mode decreases with increasing NN ligation and therefore with a decrease in the number of noble gas atoms remaining in the primary coordination sphere around the NUN molecule. We find the $NUN(NN)_5$ complex with five equatorial NN ligands to be isostructural with the $UO_2^+(CO)_5$ complex investigated recently in the gas phase.[19] Our calculations show that the $UN(N_2)_6$ complex has one axial and five equatorial NN ligands. We note that the principal NUN vibration for the supercomplex represented here by $NUN(NN)_5[NN]_x$ changes from 1000.3 cm^{-1} for a residual neon matrix shell to 997.0 cm^{-1} for a residual argon shell (using N_2 at 2.5%) and to 995.7 cm^{-1} for pure nitrogen all around. In a pure nitrogen matrix, the U atom forms the heptacoordinate $U(NN)_7$ complex, which upon UV irradiation produces the $NUN(NN)_5[NN]_x$ supercomplex with the N≡U≡N uranium dinitride core.

ASSOCIATED CONTENT

Supporting Information

Additional figures showing matrix infrared spectra using 10% $^{14}N_2$ and 8% $^{15}N_2$ in argon, using pure nitrogen, and using 0.05 and 0.2% $^{15}N_2$ in neon; additional $NU(NN)_x$ and $U(NN)_7$ calculated frequencies; a figure showing corresponding complementary W and Th nitride species; and Cartesian coordinates for the title molecules. This material is available free of charge via the Internet at http://pubs.acs.org.

AUTHOR INFORMATION

Corresponding Author

*E-mail: lsa@virginia.edu.

Present Addresses

†X.W.: Chemistry Department, Tongji University, Shanghai 200093, China.

‡G.P.K.: Optical Sciences Division, U.S. Naval Research Laboratory, 4555 Overlook Ave. SW, Washington, DC 20375.

Notes

The authors declare no competing financial interest.

ACKNOWLEDGMENTS

We gratefully acknowledge financial support from DOE Grants DE-SC0001034 and DE-SC002183 and NCSA Computing Grant CHE07-0004N, retirement funds from TIAA/CREF for L.A., and NNSFC Grants (21173158 and 21373152) to X.W.

REFERENCES

(1) Hayton, T. W.; Boncella, J. M.; Scott, B. L.; Batista, E. R.; Hay, P. J. Synthesis of Amido Analogs of the Uranyl Ion. *Science* **2005**, *310*, 1941−1943.

(2) Evans, W. J.; Kozimor, S. A.; Ziller, J. W. Molecular Octa-Uranium Rings with Alternating Nitride and Azide Bridges. *Science* **2005**, *309*, 1835−1838.

(3) Hayton, T. W. Recent Developments in Actinide−Ligand Multiple Bonding. *Chem. Commun.* **2013**, *49*, 2956−2973.

(4) Cantat, T.; Arliguie, T.; Noel, A.; Thuery, P.; Ephritikhine, M.; Le Floch, P.; Mezailles, N. The U=C Double Bond: Synthesis and Study of Uranium Nucleophilic Carbene Complexes. *J. Am. Chem. Soc.* **2009**, *131*, 963−972.

(5) Thomson, R. K.; Cantat, T.; Scott, B. L.; Morris, D. L.; Batista, E. R.; Kiplinger, J. L. Uranium Azide Photolysis Results in C−H Bond Activation and Provides Evidence for a Terminal Uranium Nitride. *Nat. Chem.* **2010**, *2*, 723−727.

(6) King, D. M.; Tuna, F.; McInnes, E. J. L.; McMaster, J.; Lewis, W.; Blake, A. J.; Liddle, S. T. Synthesis and Structure of a Terminal Uranium Nitride Complex. *Science* **2012**, *337*, 717−720.

(7) King, D. M.; Tuna, F.; McInnes, E. J. L.; McMaster, J.; Lewis, W.; Blake, A. J.; Liddle, S. T. Isolation and Characterization of a Uranium(VI)−Nitride Triple Bond. *Nat. Chem.* **2013**, *5*, 482−488.

(8) Mansell, S. M.; Farnaby, J. H.; Germeroth, A. I.; Arnold, P. L. Thermally Stable Uranium Dinitrogen Complex with Siloxide Supporting Ligands. *Organometallics* **2013**, *32*, 4214−4222.

(9) Silva, G. W. C.; Yeamans, C. B.; Sattelberger, A. P.; Hartmann, T.; Cerefice, G. S.; Czerwinski, K. R. Reaction Sequence and Kinetics of Uranium Nitride Decomposition. *Inorg. Chem.* **2009**, *48*, 10635−10642.

(10) Green, D. W.; Reedy, G. T. The Identification of UN in Ar Matrices. *J. Chem. Phys.* **1976**, *65*, 2921−2922.

(11) Hunt, R. D.; Yustein, J. T.; Andrews, L. Matrix Infrared Spectra of NUN Formed by the Insertion of Uranium Atoms into Molecular Nitrogen. *J. Chem. Phys.* **1993**, *98*, 6070−6074.

(12) Kushto, G. P.; Souter, P. F.; Andrews, L. An Infrared Spectroscopic and Quasirelativistic Theoretical Study of the Coordination and Activation of Dinitrogen by Thorium and Uranium Atoms. *J. Chem. Phys.* **1998**, *108*, 7121−7129 (ThN_2, UN_2, ThN, and UN in pure N_2).

(13) Kushto, G. P.; Souter, P. F.; Andrews, L.; Neurock, M. A Matrix Isolation FT-IR and Quasirelativistic Density Functional Theory Investigation of the Reaction Products of Laser-Ablated Uranium Atoms with NO, NO_2 and N_2O. *J. Chem. Phys.* **1997**, *106*, 5894−5903 (NUO and UN in solid argon).

(14) Zhou, M. F.; Andrews, L. Infrared Spectra and Pseudopotential Calculations for NUO^+, NUO, and NThO in Solid Neon. *J. Chem. Phys.* **1999**, *111*, 11044−11049 and references therein (also NUN in solid neon).

(15) Sankaran, K.; Sundararajan, K.; Viswanathan, K. S. A Matrix Isolation FTIR Investigation of Laser-Ablated Uranium Oxide in Argon and Nitrogen Matrices. *Bull. Mater. Sci.* **1999**, *22*, 785−790 (UN_2 and NUO dinitrogen complexes).
(16) Wang, X. F.; Andrews, L.; Vlaisavljevich, B.; Gagliardi, L. Combined Triple and Double Bonds to Uranium: The N≡U═N−H Uranimine Nitride Molecule Prepared in Solid Argon. *Inorg. Chem.* **2011**, *50*, 3826−3831.
(17) Andrews, L.; Wang, X.; Lindh, R.; Roos, B. O.; Marsden, C. J. Simple N≡UF_3 and P≡UF_3 Molecules with Triple Bonds to Uranium. *Angew. Chem., Int. Ed.* **2008**, *47*, 5366−5370.
(18) Andrews, L.; Wang, X. F.; Gong, Y.; Vlaisavljevich, B.; Gagliardi, L. Infrared Spectra and Electronic Structure Calculations for the $NUN(NN)_{1-5}$ and $NU(NN)_{1-6}$ Complexes in Solid Argon. *Inorg. Chem.* **2013**, *52*, 9989−9993.
(19) Matthew, D. J.; Morse, M. D. Resonant Two-Photon Ionization Spectroscopy of Jet-Cooled UN: Determination of the Ground State. *J. Chem. Phys.* **2013**, *138*, No. 184303.
(20) Wang, X.; Andrews, L.; Marsden, C. J. Reactions of Uranium Atoms with Ammonia: Infrared Spectra and Relativistic Calculations of the U:NH_3, H_2N−UH, and HN═UH_2 Complexes. *Chem.—Eur. J.* **2008**, *14*, 9192−9201.
(21) Lyon, J. T.; Andrews, L.; Malmqvist, P.-Å.; Roos, B. O.; Yang, T.; Bursten, B. E. Infrared Spectrum and Bonding in Uranium Methylidene Dihydride, CH_2═UH_2. *Inorg. Chem.* **2007**, *46*, 4917−4925.
(22) Roos, B. O.; Lindh, R.; Cho, H.-G.; Andrews, L. On the Agostic Interaction in the Methylidene Metal Dihydride Complexes H_2MCH_2 (M = Y, Zr, Nb, Mo, Ru, Th, or U). *J. Phys. Chem. A* **2007**, *111*, 6420−6424 (CH_2═UH_2).
(23) Wang, X.; Andrews, L.; Malmqvist, P.-Å.; Roos, B. O.; Gonçalves, A. P.; Pereira, C. C. L.; Marçalo, J.; Godart, C.; Villeroy, B. Infrared Spectra and Quantum Chemical Calculations of Uranium Carbide Molecules UC and CUC with Triple Bonds. *J. Am. Chem. Soc.* **2010**, *132*, 8484−8488 (UC, CUC).
(24) Wang, X. F.; Andrews, L.; Ma, D.; Gagliardi, L.; Gonçalves, A. P.; Pereira, C. C. L.; Marçalo, J.; Godart, C.; Villeroy, B. Infrared Spectra and Quantum Chemical Calculations of the Uranium−Carbon Molecules UC, CUC, UCH, and $U(CC)_2$. *J. Chem. Phys.* **2011**, *134*, No. 244313.
(25) Andrews, L.; Souter, P. F.; Bare, W. D.; Liang, B. Reactions of Laser-Ablated Mo and W Atoms with Dinitrogen: Infrared Spectra of Metal Nitrides, Dinitrides, and Complexes in Solid Argon and Nitrogen. *J. Phys. Chem. A* **1999**, *103*, 4649−4658.
(26) Zhou, M. F.; Andrews, L.; Li, J.; Bursten, B. E. Reactions of Laser-Ablated Uranium Atoms with CO: Infrared Spectra of the CUO, CUO^-, OUCCO, (η^2-C_2)UO_2, and $U(CO)_x$ (x = 1−6) Molecules in Solid Neon. *J. Am. Chem. Soc.* **1999**, *121*, 9712−9721.
(27) Li, J.; Bursten, B. E.; Liang, B.; Andrews, L. Noble Gas−Actinide Compounds: Complexation of the CUO Molecule by Ar, Kr, and Xe Atoms in Noble Gas Matrices. *Science* **2002**, *295*, 2242−2245.
(28) Liang, B.; Andrews, L.; Li, J.; Bursten, B. E. Noble Gas−Actinide Compounds: Evidence for the Formation of Distinct $CUO(Ar)_{4-n}(Xe)_n$ and $CUO(Ar)_{4-n}(Kr)_n$ (n = 1, 2, 3, 4) Complexes. *J. Am. Chem. Soc.* **2002**, *124*, 9016−9017.
(29) Andrews, L.; Liang, B.; Li, J.; Bursten, B. E. Noble Gas−Actinide Complexes of the CUO Molecule with Multiple Ar, Kr, and Xe Atoms in Noble-Gas Matrices. *J. Am. Chem. Soc.* **2003**, *125*, 3126−3139.
(30) Ricks, A. M.; Gagliardi, L.; Duncan, M. A. Uranium Oxo and Superoxo Cations Revealed Using Infrared Spectroscopy in the Gas Phase. *J. Am. Chem. Soc.* **2010**, *132*, 15905−15907.
(31) Hunt, R. D.; Andrews, L. Reactions of Pulsed-Laser Evaporated Uranium Atoms with Molecular Oxygen: Infrared Spectra of UO, UO_2, UO_3, UO_2^+, and UO_3−O_2 in Solid Argon. *J. Chem. Phys.* **1993**, *98*, 3690−3696 (UO_2 and UO_3).
(32) Zhou, M.; Andrews, L.; Ismail, N.; Marsden, C. Infrared Spectra of UO_2, UO_2^+, and UO_2^- in Solid Neon. *J. Phys. Chem. A* **2000**, *104*, 5495−5502.
(33) Andrews, L. Matrix Infrared Spectra and Density Functional Calculations of Transition Metal Hydrides and Dihydrogen Complexes. *Chem. Soc. Rev.* **2004**, *33*, 123−132 and references therein.
(34) Andrews, L.; Cho, H.-G. Matrix Preparation and Spectroscopic and Theoretical Investigations of Simple Methylidene and Methylidyne Complexes of Group 4, 5, and 6 Transition Metals. *Organometallics* **2006**, *25*, 4040−4053 and references therein.
(35) Frisch, M. J.; Trucks, G. W.; Schlegel, H. B.; Scuseria, G. E.; Robb, M. A.; Cheeseman, J. R.; Scalmani, G.; Barone, V.; Mennucci, B.; Petersson, G. A., et al. *Gaussian 09*, revision A.02; Gaussian, Inc.: Wallingford, CT, 2009.
(36) Becke, A. D. Density functional thermochemistry. III. The role of exact exchange. *J. Chem. Phys.* **1993**, *98*, 5648−5652.
(37) Lee, C.; Yang, Y.; Parr, R. G. Development of the Colle−Salvetti Correlation-Energy Formula into a Functional of the Electron Density. *Phys. Rev. B* **1988**, *37*, 785−789.
(38) Becke, A. D. Density-functional thermochemistry. V. Systematic optimization of exchange−correlation functionals. *J. Chem. Phys.* **1997**, *107*, 8554−8560 and references therein.
(39) Frisch, M. J.; Pople, J. A.; Binkley, J. S. Self-consistent molecular orbital methods. Supplementary functions for Gaussian basis sets. *J. Chem. Phys.* **1984**, *80*, 3265−3269.
(40) Küchle, W.; Dolg, M.; Stoll, H.; Preuss, H. Energy adjusted pseudopotentials for actinides. Parameter sets and test calculations for thorium and thorium monoxide. *J. Chem. Phys.* **1994**, *100*, 7535−7542.
(41) Roos, B. O. The Complete Active Space Self-Consistent Field Method and Its Applications in Electronic Structure Calculations. *Adv. Chem. Phys.* **1987**, *69*, 399−445.
(42) Andersson, K.; Malmqvist, P.-Å.; Roos, B. O. Second-order perturbation theory with a complete active space self-consistent field reference function. *J. Chem. Phys.* **1992**, *96*, 1218−1226.
(43) (a) Roos, B. O.; Lindh, R.; Malmqvist, P.-Å.; Veryazov, V.; Widmark, P.-O. New Relativistic ANO Basis Sets for Transition Metal Atoms. *J. Phys. Chem. A* **2005**, *109*, 6575−6579 (ANO-RCC-VTZP basis set). (b) Karlström, G.; Lindh, R.; Malmqvist, P.-Å.; Roos, B. O.; Ryde, U.; Veryazov, V.; Widmark, P.-O.; Cossi, M.; Schimmelpfennig, B.; Neogrady, P.; Seijo, L. MOLCAS: A program package for computational chemistry. *Comput. Mater. Sci.* **2003**, *28*, 222−239.
(44) Huber, K. P.; Herzberg, G. *Constants of Diatomic Molecules*; Van Nostrand Reinhold: New York, 1979.
(45) Berthet, J.-C.; Thuery, P.; Ephritikhine, M. The First Actinyl Cyanide. *Chem. Commun.* **2007**, 604−606.
(46) Maynadie, J.; Barros, N.; Berthet, J.-C.; Thuery, P.; Maron, L.; Ephritikhine, M. The Crucial Role of f Electrons in the Bent or Linear Configuration of Uranium Cyanido Metallocenes. *Angew. Chem., Int. Ed.* **2007**, *46*, 2010−2102.
(47) Thompson, W. E.; Jacox, M. E. The Vibrational Spectra of Molecular Ions Isolated in Solid Neon. III. N_4^+. *J. Chem. Phys.* **1990**, *93*, 3856−3862.
(48) Jacox, M. E. The Vibrational Levels of Small Transient Molecules Isolated in Neon and Argon Matrices. *Chem. Phys.* **1994**, *189*, 149−170.
(49) Vlaisavljevich, B.; Gagliardi, L.; Wang, X. F.; Liang, B.; Andrews, L. U and P_4 Reaction Products: A Quantum Chemical and Matrix Isolation Spectroscopic Investigation. *Inorg. Chem.* **2010**, *49*, 9230−9235 and references therein (also comparisons of UN, UP, NUN, and PUP at the CASPT2 level).
(50) Ma, D.; Li Manni, G.; Gagliardi, L. The Generalized Active Space Concept in Multiconfigurational Self-Consistent Field Methods. *J. Chem. Phys.* **2011**, *135*, No. 044128.
(51) Straka, M.; Patzschke, M.; Pyykkö, P. Why Are Hexavalent Uranium Cyanides Rare While U−F and U−O Bonds Are Common and Short? *Theor. Chem. Acc.* **2003**, *109*, 332−340.
(52) Work in progress in this laboratory has characterized $U(NC)_{1,2,4}$ molecules in the reaction of U atom with cyanogen using isotopic substitutions, and calculations have shown that the isolated isocyanides are more stable than the analogous cyanides of uranium. See: Andrews, L.; Gong, Y.; Garner, E. B., III; Dixon, D. A. To be submitted.

(53) Gagliardi, L.; Pyykkö, P. Theoretical Search for Very Short Metal−Actinide Bonds: NUIr and Isoelectronic Systems. *Angew. Chem., Int. Ed.* **2004**, *43*, 1573−1576.
(54) Sattelberger, A. P.; Johnson, M. J. A. Uncovering the Uranium−Nitrogen Triple Bond. *Science* **2012**, *337*, 652−653.